On symmetry breaking in BNB: Real or artifactual?

Apostolos Kalemos and Thom H. Dunning, Jr.[a)]
Joint Institute for Computational Sciences, University of Tennessee–Oak Ridge National Laboratory, Oak Ridge, Tennessee 37831, Department of Chemistry, University of Tennessee, Knoxville, Tennessee 37996, and Computer Science and Mathematics Division, Oak Ridge National Laboratory, Oak Ridge, Tennessee 37831

Aristides Mavridis
Laboratory of Physical Chemistry, Department of Chemistry, National and Kapodistrian University of Athens, P.O. Box 64004, 157 10 Zografou, Athens, Greece

(Received 5 August 2003; accepted 31 October 2003)

The ground state of the linear BNB molecule has been examined with multireference-based *ab initio* methods coupled with quantitative basis sets. Previous computational studies on BNB, even those using highly correlated single reference-based methods, e.g., the CCSD(T) and BDT methods, suggested that the two BN bond lengths were unequal. In this paper, the $BN(X\,^3\Pi)+B(^2P_u)$ potential energy curve is constructed using a state-averaged multireference-based correlated method (SA-CASSCF+PT2). The four lowest states of BN were included in the state averaging procedure. These calculations reveal no symmetry breaking along the antisymmetric stretching mode of the molecule. © *2004 American Institute of Physics.* [DOI: 10.1063/1.1635797]

I. INTRODUCTION

Boron nitride clusters, B_xN_y, have recently received considerable attention due to the favorable properties and industrial applications of boron nitride thin films[1] formed by such clusters. One of the simplest boron–nitrogen containing entities is the triatomic BNB molecule, a major product observed in laser ablation studies of solid boron nitride.[2,3] Since the identification of BNB in the late 1980s, several theoretical and experimental studies appeared questioning the linear centrosymmetric structure of its ground state.[4–17]

The first *ab initio* study was that of Martin *et al.*,[4] who, based on an UHF/6-31G* geometry optimization, predicted that the symmetry of the ground state was $^2\Sigma_u^+$ (cf. Table I). It should be noted, however, that the UHF wave function was constrained to conform to $D_{\infty h}$ point group symmetry. The first experimental investigation,[6] a matrix ESR study, yielded spectroscopic evidence for a linear symmetric BNB structure of $^2\Sigma_u^+$ symmetry, in accordance with the theoretical study.[4] Geometry optimizations[6] at MP2, MP4, and CISD levels of theory for a $D_{\infty h}$ structure yielded calculated nuclear hyperfine parameters, in excellent agreement with the experimental values.[6]

A cyclic C_{2v} ground state structure emerged from isotopic studies using laser evaporation techniques[8] and subsequent theoretical investigations[9] reported a cyclic isomer of BNB. The authors claimed that the strong fundamental observed at 882.3 cm^{-1}, and attributed to the antisymmetric B–N stretching mode, was too low and had inappropriate isotopic shifts for a linear structure.[9] Moreover, a potential energy surface search at the HF/6-31G* level revealed a low lying $^2B_2$ state located 1.6 kcal/mol above the $\tilde{X}\,^2\Sigma_u^+$ state at the QCISD(T)/6-31G*//HF/6-31G* level of theory (cf. Table I). The absence of the $^2B_2$ state in the ESR experiments[6] was attributed[9] to experimental differences in the generation of the molecule and relaxation of the energized evaporated species. In a recent B3LYP/6-31G(d) study of the $B+NH_3$ reaction products,[13] the existence of a cyclic $^2B_2$ state was strongly questioned, instead, a $^2A_1$ state was proposed lying 40.6 kcal/mol above the $\tilde{X}$ state.

A theoretical study by Martin *et al.*,[12] based on a full valence CASSCF ($11e^-$/12 orbitals)/cc-pV(D,T)Z wave function, exhibited symmetry breaking (SB) along the antisymmetric B–N stretching coordinate, giving rise to a $C_{\infty v}$ geometry for the ground state. The authors maintained that the SB was genuine rather than artificial, but they did not exclude the possibility that a more ''physical'' $D_{\infty h}$ structure would be obtained at higher correlated levels of theory.

In a photoelectron spectroscopic study of B_2N^-, Asmis *et al.*[14(b)] suggested a linear symmetric structure for both the ground and first excited states of BNB, while no evidence of a low-lying cyclic isomer was detected. Theoretical results based on the DFT and coupled cluster (CC) methodologies were interpreted as supporting the $D_{\infty h}$ structure, even though the computed *ab initio* potential energy curves (PECs) exhibited SB effects.[14(b)] Following their study more closely, we note that a Herzberg–Teller vibronic coupling between the $\tilde{X}\,^2\Sigma_u^+$ and the $\tilde{A}\,^2\Sigma_g^+$ states via the Q_3 (antisymmetric B–N stretching) mode is possible, but it is not expected to be strong enough to create a dipolar distortion. Both computational approaches (DFT and CC) gave no evidence for a $^2B_2$ minimum. A $^4B_2$ state appeared at 2.120 (1.943) eV at the B3LYP/aug-cc-pVTZ[CCSD(T)/aug-cc-pVTZ] level of theory and was identified as the lowest lying stable cyclic isomer (cf. Table I).[14(b)]

In an effort to resolve the ambiguity of whether the lin-

a)Electronic mail: dunning@jics.utk.edu

TABLE I. Total energies E_e (hartree), atomization energies AE_e (kcal/mol), bond distances r_e (Å), angles θ_e (°), harmonic frequencies $\omega_{1,2,3}$ (cm^{-1}), and energy separations T_e (kcal/mol) of existing theoretical and experimental results on various BNB states.

State	E_e	AE_e	r_e	θ_e	ω_1	ω_2	ω_3	T_e (kcal/mol)
$\tilde{X}\,^2\Sigma_u^+$	−104.013 75[a]	239.50[a]	1.309[d]		1108(σ_g)[d]	73(π_u)[d]	2021(σ_u)[d]	0.0
	−104.006 72[b]	269.7±4[c]						0.0
	−104.009 85[e]		1.338[e]					0.0
		255.7±2[f]	1.327[g]		1183(σ_g)[g]	153(π_u)[g]	2392(σ_u)[g]	0.0
	−104.009 31[h]		1.309[i]		1245(σ_g)[i]	82(π_u)[i]	2271(σ_u)[i]	0.0
					1149(σ_g)[l]	147.9(π_u)[l]	1279.4(σ_u)[l]	0.0
	−104.356 32[m]		1.312		1196(σ_g)	124(π_u)	1327(σ_u)	0.0
	−104.106 48[n]		1.328		1143(σ_g)	85(π_u)	1320i(σ_u)	0.0
					1143±40(σ_g)[o]		855±40(σ_u)[o]	0.0
	−104.140 259[p]		1.320[p]					161±20 cm^{-1}[p]
$^2B_2$	−104.006 76[h]		1.325[i]	81.5[i]	1608(α_1)[i]	643(α_1)[i]	1178(b_2)[i]	1.6[h]
					1116(α_1)[j]		882.3(b_2)[j]	
$^2\Sigma_g^+$	−103.982 10[h]		1.292[i]		1352(σ_g)[i]	440(π_u)[i]	2224(σ_u)[i]	17.1[h]
			1.298[m]		1270(σ_g)	126(π_u)	2324i(σ_u)	13.6
			1.314[n]					16.1
					1174±40(σ_g)[o]		2492±40(σ_u)[o]	18.1±0.1[o]
$^2\Sigma^+$			1.4023[k]		1062(σ)	146(π)	1865(σ)	
			1.2738[k]					
			1.280[n]		1052(σ)	339(π)	1683(σ)	0.65
			1.383[n]					
	−104.140 926[p]		1.278[p]					0.0[p]
			1.367[p]					
$^2A_1$			1.380[l]	65.8	1471.6(α_1)	1073(α_1)	965.9(b_2)	40.6
$^4B_2$			1.379[m]	77.8	1408(α_1)	732(α_1)	1189(b_2)	48.9
			1.395[n]	77.0	1367(α_1)	746(α_1)	1158(b_2)	44.8

[a]Projected UMP4/6-31G*//UHF/6-31G*, Ref. 4.
[b]CCD+ST(CCD)/6-31G*, Ref. 4.
[c]CCD+ST(CCD)/6-31G* binding energy scaled by 1.15, Ref. 4.
[d]UHF/6-31G* level of theory, harmonic frequencies scaled by 0.89, Ref. 4.
[e]MP4/6-31G*, Ref. 6.
[f]G1 estimate, Ref. 7.
[g]MP2/6-31G*, Ref. 7.
[h]QCISD(T)/6-31G*, Ref. 9.
[i]HF/6-31G*, Ref. 9.
[j]Exp, IR fundamentals, Ref. 9.
[k]CASSCF(11e^-12orb)/cc-pVTZ, Ref. 12.
[l]B3LYP/6-31G(d), Ref. 13.
[m]B3LYP/aug-cc-pVTZ, Ref. 14(b).
[n]CCSD(T)/aug-cc-pVTZ, Ref. 14(b).
[o]Photoelectron spectroscopy; the quoted number 855±40 cm^{-1}, refers to the bending fundamental; Ref. 14(b).
[p]Extrapolated from QRHF-CCSD(T)/cc-pVnZ, $n=2$, 3, 4, Ref. 16.

ear structure was symmetric or not, Asmis *et al.*[14(b)] employed both DFT and CC methods and constructed PECs along Q_3, the antisymmetric stretch coordinate. The B3LYP/aug-cc-pVTZ calculations predicted a single well with a $D_{\infty h}$ minimum, but the resulting harmonic frequency of the Q_3 mode was not in agreement with the experimental value. On the other hand, the single reference correlated approaches CCSD and CCSD(T) displayed double wells with singularities at the $D_{\infty h}$ structure. The SB problem was subsequently tackled using Brueckner orbitals within the CC method. Although the resulting PEC [BD(T)/cc-pVDZ] did not give a realistic topology, the ''asymmetry'' was quite small and smoothed fits of the PEC reproduced the experimentally observed vibrational levels.

Since the experimental findings of Asmis *et al.*[14(b)] suggested a breakdown of the Born–Oppenheimer approximation, a linear vibronic coupling model was applied in order to explain the low ν_3 fundamental frequency.[14(b)] This model resulted in a $C_{\infty v}$ structure for the $\tilde{X}$ state with a barrier to a $D_{\infty h}$ structure of merely 18 cm^{-1}, very small in comparison to the zero point energy of 355 cm^{-1} for the Q_3 mode. The authors concluded that the ground state is an intermediate case of symmetry breaking with a quasisymmetric structure. No conclusions could be drawn from the *ab initio* results since these were contaminated by SB effects.

The last theoretical account aimed at elucidating the existence or not of a symmetric linear structure and/or the presence of a cyclic isomer for the ground state of BNB is that of Gwaltney and Head-Gordon.[16] Employing three different variants of the CC methodology, i.e., CCSD, CCSD(T), and CCSDT, based on both HF and Brueckner orbitals, they concluded that the BNB molecule is indeed linear and undergoes a real pseudo Jahn–Teller effect with a barrier to the centrosymmetric structure of 161±20 cm^{-1} (well below the first vibrational level), and a bond length difference between the two B–N bonds of 0.09 Å (cf. Table I). The equivalence of the boron atoms predicted by the ESR experiment[6] was justified on the basis of the zero point motion, which is fast

compared to the time scale of the experiment. It was concluded that the BNB molecule is linear but very floppy and with a quasi centrosymmetric structure, representing one of the most insidious examples of SB effects discovered.[16]

Twenty years ago, Davidson and Borden, in a Feature Article in the Journal of Physical Chemistry,[18] stated that one of the most common reasons that a symmetry broken solution might appear as a minimum on a calculated potential surface is that the calculations are wrong. Symmetry breaking takes place when there is a triggering mechanism that lowers the energy when the symmetry is reduced, and is always associated with a degeneracy or near degeneracy.[19] In cases of a real SB effect the triggering mechanism is vibronic coupling (Jahn–Teller vibronic coupling effects), while in cases of artificial SB effects the source of the problem stems from the oversimplified nature of the adopted wave function.[18]

The nonadiabatic equations in the strong coupling limit of a pseudo-Jahn–Teller case in linear centrosymmetric molecules allow for breakdown of the g/u symmetry and the creation of a dipole moment.[19] But, it is often very difficult to distinguish real from artificial symmetry breaking. Although it is possible to correct cases of artificial symmetry breaking by using highly correlated wave functions, especially those based on Brueckner orbitals, it is not always possible to do so using single reference configuration approaches.

II. COMPUTATIONAL DETAILS

In an effort to resolve the conundrum of the BNB system, we explored the use of CASSCF wave functions as a reference for subsequent dynamical correlation treatments and calculated the energy along the BN–B coordinate. The active space for the CASSCF wave function was composed of all the valence orbitals of the constituent atoms, i.e., $2s+2p$. This provides a balanced space for all 11 valence BNB electrons. Four states of $^2\Sigma^+$ symmetry, resulting from the interaction $\mathrm{BN}(^{1,3}\Sigma^+,^{1,3}\Pi)+\mathrm{B}(^2P_u)$, were state averaged during the CASSCF optimization step; the reason for this choice is discussed in the following section. The number of configuration functions (CF) resulting from such a distribution is 85 428 of $^2A_1$ symmetry, with the CASSCF wave functions displaying axial angular momentum symmetry with $|\Lambda|=0(\Sigma^+)$.

The valence correlation energy was computed using second-order Rayleigh–Schrödinger perturbation theory (RSPT2) for every point of the BN+B interaction curve. Use of the more computationally demanding MRCI (CASSCF +1+2) method was limited to the construction of the BN molecule's PECs and to the optimization of the BNB ground-state geometry. The one electron orbital space was generated using the cc-pVQZ basis set[20] for both B and N atoms. All computations are carried out with the MOLPRO suite of programs.[21]

III. CHARACTERIZATION OF BN

The details of the formation of the BNB molecule from its fragments should not be overlooked if one wants to obtain insight into the symmetry-breaking (SB) problem as well as to determine a way to construct a wave function that does not give rise to the anomalies found earlier. Let us consider the BN+B interaction in some detail. The low-lying states of BN, those within 1 eV of the ground state, are the $X\,^3\Pi$, $a\,^1\Sigma^+$, $b\,^1\Pi$, $A\,^3\Sigma^+$ and $B\,^3\Sigma^-$ states. MRCI PECs for these states are displayed in Fig. 1 with the corresponding spectroscopic parameters listed in Table II. As can be seen from Fig. 1, the $X\,^3\Pi$ and $B\,^3\Sigma^-$ states dissociate adiabatically to ground state atoms, while the rest of the states dissociate to the first excited state, ^2D_u, of the nitrogen atom.

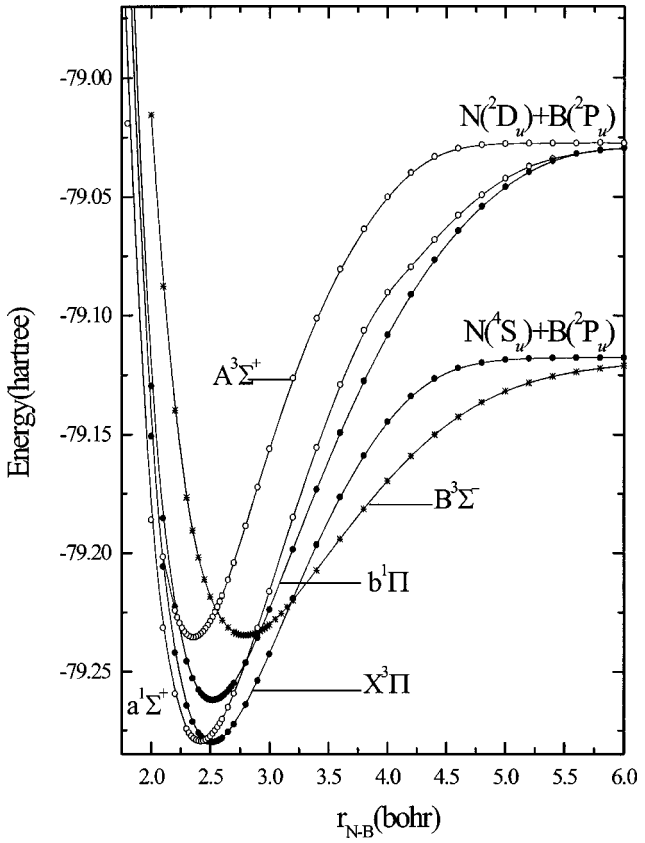

FIG. 1. Potential energy curves of the $X\,^3\Pi$, $a\,^1\Sigma^+$, $b\,^1\Pi$, $A\,^3\Sigma^+$, and $B\,^3\Sigma^-$ states of BN at the MRCI/cc-pVQZ level of theory.

In Table III we summarize the characteristics of the above states at their equilibrium bond lengths, listing the leading molecular orbital configurations, (valence) molecular orbital compositions, and Mulliken atomic distributions. We observe that, in all but the $B\,^3\Sigma^-$ state, the *in situ* B atom is in the excited ^4P_g state, while N is in its ground ^4S_u state, irrespective of the dissociation products. The essential physics of the N+B interaction is captured in the following valence-bond-Lewis (vbL) diagrams:

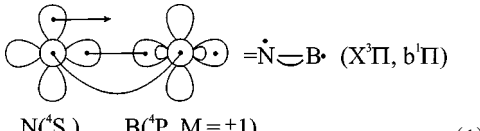

(1)

TABLE II. Total energies E_e (hartree), bond lengths r_e (Å), dissociation energies D_e (kcal/mol), dipole moments μ_e (D), zero-point energies ZPE (cm^{-1}), and energy separations T_e (kcal/mol) of the $X\,^3\Pi$, $a\,^1\Sigma^+$, $b\,^1\Pi$, $A\,^3\Sigma^+$, and $B\,^3\Sigma^-$ $^{11}B^{14}N$ states at the MRCI level of theory. Experimental values in parentheses.

State	E_e	r_e	D_e[a]	μ_e	ZPE[b]	T_e
$X\,^3\Pi$	−79.279 971	1.330 (1.329)[c]	102.2	1.948	754.57 (756.45)[e]	0.0
$a\,^1\Sigma^+$	−79.279 534	1.279 (1.274±0.005)[d]	158.8	1.908	847.65 (847.98)[e]	0.27 (0.44)[d]
$b\,^1\Pi$	−79.262 110	1.333 (1.330±0.005)[d]	147.6	2.201	760.06 (763.48)[e]	11.21 (10.77)[d]
$A\,^3\Sigma^+$	−79.235 474	1.247	130.8	0.687	905.46 (909.85)[e]	27.92 (27.72)[d]
$B\,^3\Sigma^-$	−79.234 665	1.479	73.7	0.603	535.74 (534.8)[e]	28.43 (29.54)[e]

[a]Dissociation energy with respect to the adiabatic fragments.
[b]ZPE$=1/2\omega_e-1/4\omega_e x_e$.
[c]r_o value, Ref. 22; for a discussion of the best r_e estimate ($r_e=1.325\pm0.002$ Å), see Ref. 23.
[d]Reference 24.
[e]Reference 25.

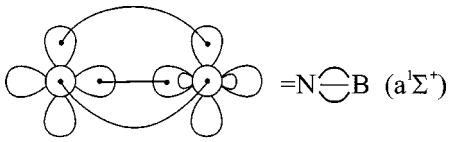

(2)

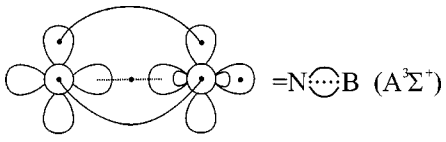

(3)

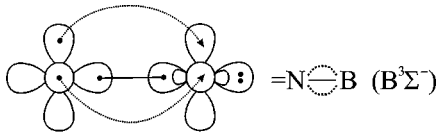

(4)

Upon interaction with a second B atom in its ground $^2P_u(2s^22p^1)$ state along a $C_{\infty v}$ approach from the N end, all but the $B\,^3\Sigma^-$ state can form a $^2\Sigma^+$ BNB state, which at the $D_{\infty h}$ nuclear configuration will be of either "*u*" or "*g*" symmetry. Along the $C_{\infty v}$ reaction coordinate all four $^2\Sigma^+$ BN···B states can variationally interact, but at the centrosymmetric geometry the interaction is limited among the "*u*" or "*g*" spaces.

It is clear from the vbL icons (1)–(3) that, in BNB, one B atom, the one in the BN molecule, would be *in situ* excited, while the other B atom, the one approaching the BN molecule, would be in its ground state. At the $D_{\infty h}$ geometry, no distinction should exist between the two B atoms. However, this requires a carefully constructed wave function. Single reference wave functions have proven to be unstable with respect to antisymmetric stretching. Correlation treatments based on such reference functions could not recover from the SB problem;[14(b),16] even a full valence CASSCF treatment seems to suffer from the same illness.[12]

One could also consider the formation of BNB from B_2+N. With this, we reach the same qualitative conclusions as before. A B_2 molecular state that dissociates into $B(^2P_u)+B(^4P_g)$ should be described by a multiconfigurational reference wave function that accounts for the "resonance" degeneracy. In valence bond language this means that at infinity the $B(^2P_u)+B(^4P_g)$ and $B(^4P_g)+B(^2P_u)$ configurations should both be represented in the wave function. A nitrogen atom, $N(^4S_u)$ in the middle of the molecule, does

TABLE III. Configurations, orbital compositions, and atomic populations for the first five states of BN at their respective equilibrium geometries.

State	Configuration	Orbitals	Atomic populations	Asymptotic atomic populations
$X\,^3\Pi(^3B_1)$	$0.96\|1\sigma^2 2\sigma^2 3\sigma^1 1\pi_x^1 1\pi_y^2\rangle$	$1\sigma\sim0.96(2s)_N+0.23(2s)_B-0.25(2p_z)_B$ $2\sigma\sim0.77(2p_z)_N+0.70(2s)_B-0.36(2p_z)_B$ $3\sigma\sim0.36(2p_z)_N-0.64(2s)_B-0.74(2p_z)_B$ $1\pi\sim0.76(2p_\pi)_N+0.52(2p_\pi)_B$	N: $2s^{1.74}2p_z^{1.41}2p_x^{0.69}2p_y^{1.31}$ B: $2s^{1.15}2p_z^{0.64}2p_x^{0.30}2p_y^{0.63}$	N: $2s^{2.0}2p_z^{1.0}2p_x^{1.0}2p_y^{1.0}$ B: $2s^{1.89}2p_z^{0.06}2p_x^{0.05}2p_y^{1.0}$
$a\,^1\Sigma^+(^1A_1)$	$0.88\|1\sigma^2 2\sigma^2 1\pi_x^2 1\pi_y^2\rangle$ $-0.31\|1\sigma^2 3\sigma^2 1\pi_x^2 1\pi_y^2\rangle$	$1\sigma\sim0.86(2s)_N+0.24(2p_z)_N+0.47(2s)_B-0.38(2p_z)_B$ $2\sigma\sim0.43(2s)-0.57(2p_z)_N-0.77(2s)_B$ $3\sigma\sim0.73(2p_z)_N-0.48(2s)_B-0.65(2p_z)_B$ $1\pi\sim0.76(2p_\pi)_N+0.56(2p_\pi)_B$	N: $2s^{1.59}2p_z^{0.92}2p_x^{1.31}2p_y^{1.31}$ B: $2s^{1.0}2p_z^{0.45}2p_x^{0.65}2p_y^{0.65}$	N: $2s^{2.0}2p_z^{1.0}2p_x^{1.0}2p_y^{1.0}$ B: $2s^{1.89}2p_z^{0.06}2p_x^{0.53}2p_y^{0.53}$
$b\,^1\Pi(^1B_1)$	$0.96\|1\sigma^2 2\sigma^2 3\sigma^1 1\pi_x^1 1\pi_y^2\rangle$	$1\sigma\sim0.96(2s)_N+0.18(2s)_B-0.21(2p_z)_B$ $2\sigma\sim0.77(2p_z)_N+0.71(2s)_B-0.41(2p_z)_B$ $3\sigma\sim0.31(2p_z)_N-0.64(2s)_B-0.76(2p_z)_B$ $1\pi\sim0.86(2p_\pi)_N+0.40(2p_\pi)_B$	N: $2s^{1.72}2p_z^{1.41}2p_x^{0.78}2p_y^{1.27}$ B: $2s^{1.12}2p_z^{0.68}2p_x^{0.20}2p_y^{0.66}$	N: $2s^{2.0}2p_z^{1.0}2p_x^{1.0}2p_y^{1.0}$ B: $2s^{1.89}2p_z^{0.06}2p_x^{0.05}2p_y^{1.0}$
$A\,^3\Sigma^+(^3A_1)$	$0.96\|1\sigma^2 2\sigma^1 3\sigma^1 1\pi_x^2 1\pi_y^2\rangle$	$1\sigma\sim0.85(2s)_N+0.27(2p_z)_N+0.49(2s)_B-0.41(2p_z)_B$ $2\sigma\sim0.45(2s)-0.57(2p_z)_N-0.76(2s)_B-0.13(2p_z)_B$ $3\sigma\sim0.15(2s)-0.66(2p_z)_N+0.33(2s)_B+0.78(2p_z)_B$ $1\pi\sim0.78(2p_\pi)_N+0.53(2p_\pi)_B$	N: $2s^{1.49}2p_z^{0.84}2p_x^{1.38}2p_y^{1.38}$ B: $2s^{1.0}2p_z^{0.65}2p_x^{0.57}2p_y^{0.57}$	N: $2s^{2.0}2p_z^{1.0}2p_x^{1.0}2p_y^{1.0}$ B: $2s^{1.89}2p_z^{0.06}2p_x^{0.53}2p_y^{0.53}$
$B\,^3\Sigma^-(^3A_2)$	$0.96\|1\sigma^2 2\sigma^2 3\sigma^1 1\pi_x^1 1\pi_y^1\rangle$	$1\sigma\sim0.90(2s)_N-0.41(2p_z)_N$ $2\sigma\sim0.34(2s)_N+0.72(2p_z)_N+0.47(2s)_B-0.52(2p_z)_B$ $3\sigma\sim0.14(2s)_N+0.14(2p_z)_N-0.84(2s)_B-0.51(2p_z)_B$ $1\pi\sim0.90(2p_\pi)_N+0.27(2p_\pi)_B$	N: $2s^{1.80}2p_z^{1.50}2p_x^{0.89}2p_y^{0.89}$ B: $2s^{1.77}2p_z^{0.74}2p_x^{0.16}2p_y^{0.16}$	N: $2s^{2.0}2p_z^{1.0}2p_x^{1.0}2p_y^{1.0}$ B: $2s^{1.89}2p_z^{1.0}2p_x^{0.05}2p_y^{0.05}$

TABLE IV. Total energies E_e (hartree), equilibrium bond lengths r_e (Å), and dipole moments μ_e (D) of the ground $\tilde{X}\,^2\Sigma_u^+$ state of BNB at various levels of theory.

Method	E_e	r_e (B_1N)	r_e (NB_2)	μ_e
CASSCF+PT2[a]	−104.110 217	1.275	1.381	3.58
SACASSCF+PT2	−104.115 799	1.325	1.325	0.0
CASSCF+1+2[a]	−104.113 720	1.273	1.381	3.66
SACASSCF+1+2	−104.112 996	1.324	1.324	0.0

[a]$C_{\infty v}$ point group symmetry.

not change the symmetry requirements that need to be obeyed.

IV. RESULTS AND DISCUSSION

Table IV presents the equilibrium energies (E_e), bond lengths (r_e), and dipole moments (μ_e) of the $\tilde{X}$ BNB state at different levels of theory, while Fig. 2 displays part of the PEC for the $BN(X\,^3\Pi)+B(^2P_u)$ interaction; Fig. 3 shows the energy as a function of $r_{NB_1}-r_{NB_2}$ where $r_{B_1B_2}$ stays constant. Both curves were computed with the SA-CASSCF +PT2 method.

The CASSCF+1+2 (MRCI), and CASSCF+PT2 results both predict a $C_{\infty v}$ structure, while the SA-CASSCF-based correlation treatments predict a $D_{\infty h}$ structure. To better understand the reasons for this behavior, let us examine the details of the CASSCF and SA-CASSCF wave functions. At the equilibrium geometry predicted by the SA-CASSCF +PT2 wave function, the CASSCF wave function is

$$|^2\Sigma^+(^2A_1)\rangle \sim 0.93|1\sigma^2 2\sigma^2 3\sigma^2 4\sigma^1 1\pi_x^2 1\pi_y^2\rangle - 0.15|1\sigma^2 2\sigma^2(2\pi_x^2+2\pi_y^2)4\sigma^1 1\pi_x^2 1\pi_y^2\rangle,$$

with

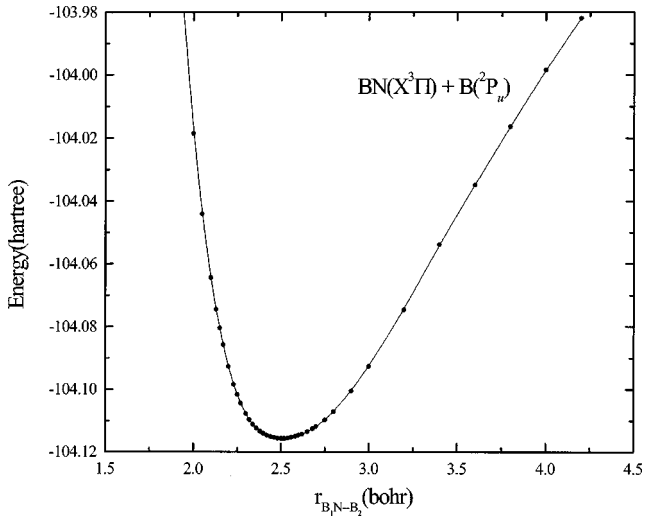

FIG. 2. Potential energy curve for the $BN(X\,^3\Pi)+B(^2P_u, M_L=\pm 1)$ interaction at the SA-CASSCF+PT2/cc-pVQZ level of theory. The BN distance has been optimized for each value of the BN–B distance.

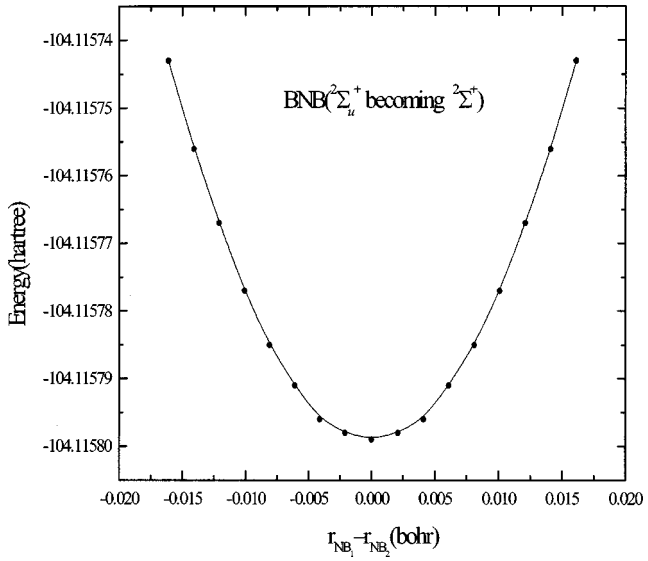

FIG. 3. The potential energy curve of the ground B_1NB_2 state as a function of the $r_{NB_1}-r_{NB_2}$ with $r_{B_1B_2}$ being held constant, at the SA-CASSCF+PT2/cc-pVQZ level of theory.

$$1\sigma \sim -0.88(2s)_N - 0.21(2s)_{B1} + 0.20(2p_z)_{B1} - 0.35(2s)_{B2} - 0.34(2p_z)_{B2},$$

$$2\sigma \sim 0.74(2p_z)_N + 0.61(2s)_{B1} - 0.42(2p_z)_{B1} - 0.37(2s)_{B2} - 0.37(2p_z)_{B2},$$

$$3\sigma \sim 0.77(2s)_{B2} - 0.53(2p_z)_{B2},$$

$$4\sigma \sim 0.70(2s)_{B1} + 0.71(2p_z)_{B1},$$

$$1\pi \sim 0.74(2p_\pi)_N + 0.42(2p_\pi)_{B1} + 0.26(2p_\pi)_{B2},$$

$$2\pi \sim 0.45(2p_\pi)_{B1} - 0.84(2p_\pi)_{B2},$$

and corresponding atomic Mulliken distributions:

$$N:\ 2s^{1.35}2p_z^{1.09}2p_x^{1.32}2p_y^{1.32},$$

$$B_1:\ 2s^{1.13}2p_z^{0.71}2p_x^{0.43}2p_y^{0.43},$$

$$B_2:\ 2s^{1.77}2p_z^{0.78}2p_x^{0.22}2p_y^{0.22}.$$

It is clear from the data above that the CASSCF wave function does not properly describe the molecule at the symmetric nuclear configuration. The two B atoms are inequivalent—one of the B atoms, B_1, is in an excited atomic state, since its $2s^{1.13}2p^{1.57}$ occupancy is indicative of a $^4P_g(2s^12p^2)$ distribution, while the second one, $B_2(2s^{1.77}2p^{1.22})$, is in its ground $^2P_u(2s^22p^1)$ state. It is a symmetry broken solution. The value of the dipole moment is 4.03 D. Electron correlation effects taken into account through the PT2 or MRCI calculations are not able to correct

the problem and the final wave function does not have the proper $D_{\infty h}$ symmetry. Hence, a CASSCF+1+2 wave function does not provide an appropriate description of the molecule.

On the other hand, the SA-CASSCF+1+2 and SA-CASSCF+PT2 wave functions do behave properly at $D_{\infty h}$ configurations (μ=0.0 D in both cases). The reference function at the symmetric minimum is

$$|^2\Sigma_u^+(^2A_1)\rangle \sim 0.91|1\sigma^2 2\sigma^2 3\sigma^2 4\sigma^1 1\pi_x^2 1\pi_y^2\rangle - 0.14|1\sigma^2 2\sigma^2 3\sigma^1 4\sigma^2(1\bar{\pi}_x^1 2\pi_x^1 1\pi_y^2 + 1\pi_x^2 1\bar{\pi}_y^1 2\pi_y^1)\rangle + 0.12|1\sigma^2 2\sigma^2 3\sigma^1 4\sigma^2(1\pi_x^2 1\pi_y^1 2\bar{\pi}_y^1 + 1\pi_x^1 2\bar{\pi}_x^1 1\pi_y^2)\rangle,$$

with

$$1\sigma \sim 0.89(2s)_N + 0.30(2s)_{B1} - 0.25(2p_z)_{B1} + 0.30(2s)_{B2} + 0.25(2p_z)_{B2},$$

$$2\sigma \sim 0.74(2p_z)_N + 0.53(2s)_{B1} - 0.35(2p_z)_{B1} - 0.53(2s)_{B2} - 0.35(2p_z)_{B2},$$

$$3\sigma \sim 0.27(2s)_N - 0.56(2s)_{B1} - 0.38(2p_z)_{B1} - 0.56(2s)_{B2} + 0.38(2p_z)_{B2},$$

$$4\sigma \sim 0.35(2p_z)_N - 0.43(2s)_{B1} - 0.52(2p_z)_{B1} + 0.43(2s)_{B2} - 0.52(2p_z)_{B2},$$

$$1\pi \sim 0.77(2p_\pi)_N + 0.33(2p_\pi)_{B1} + 0.33(2p_\pi)_{B2},$$

$$2\pi \sim 0.72(2p_\pi)_{B1} - 0.72(2p_\pi)_{B2},$$

and corresponding atomic Mulliken populations,

$$\text{N: } 2s^{1.37}2p_z^{1.10}2p_x^{1.30}2p_y^{1.30},$$

$$\text{B}_1\text{: } 2s^{1.49}2p_z^{0.70}2p_x^{0.33}2p_y^{0.33},$$

$$\text{B}_2\text{: } 2s^{1.49}2p_z^{0.70}2p_x^{0.33}2p_y^{0.33}.$$

The atomic distributions of the *in situ* B_1 and B_2 atoms indicate that each of them is an average of $B(^2P_u)$ $+B(^4P_g)$ since they are close to the average of the corresponding atomic populations of the symmetry broken CASSCF solution. Thus, the SA-CASSCF wave function, but not the CASSCF wave function, incorporates the components necessary to properly describe the symmetric $D_{\infty h}$ nuclear configuration of BNB.

In constructing the potential energy curve in Fig. 2, the BN distance was optimized for each value of the BN–B separation. Due to technical problems we were unable to converge the SA-CASSCF+PT2 calculations beyond 4.2 bohr. The minimum of this curve occurs at r_{BN}=1.325 Å [practically (1.275+1.381)/2=1.328 Å; see Table IV] and no SB effects, leading to a dipolar distortion, appear, as evidenced in Fig. 3. The dissociation energy of BNB($\tilde{X}\,^2\Sigma_u^+$) with respect to BN($X\,^3\Pi$)+B(^2P_u) is 152.1 kcal/mol, while that of the diatomic BN($X\,^3\Pi$) is 102.2 kcal/mol, at the MRCI level of theory. Hence, the calculated atomization energy of BNB($\tilde{X}\,^2\Sigma_u^+$)$\rightarrow$N(^4S_u)+2B(^2P_u) is 254.3 kcal/mol.

V. CONCLUSIONS

The $\tilde{X}\,^2\Sigma_u^+$ state of the linear BNB molecule has been examined using several *ab initio* methods based on multireference wave functions. CASSCF calculations predict a symmetry-broken (SB) structure for BNB with unequal bond lengths, as do perturbation theory (CASSCF+PT2) and multireference CI (CASSCF+1+2) wave functions based on the CASSCF wave function. A state-averaged CASSCF wave function, SA-CASSCF, predicts a symmetric structure for BNB, as do the resulting SA-CASSCF-PT2 and SA-CASSCF+1+2 calculations. The four lowest-lying states of BN($X\,^3\Pi, a\,^1\Sigma^+, b\,^1\Pi, A\,^3\Sigma^+$), all of which can interact strongly along the BN–B coordinate, were included in the state averaging procedure.

An analysis of the CASSCF wave function shows that, in the $\tilde{X}$ state of the BNB molecule, one B atom is *in situ* excited (^4P_g), while the other is in its ground state (^2P_u), or, schematically, B*–N–B. Since quantum-mechanically the B atoms must be indistinguishable at the $D_{\infty h}$ nuclear configuration, the wave function must describe B–N–B* and B*–N–B equally well. The inclusion of dynamical electron correlation effects using either the CASSCF+PT2 and CASSCF+1+2 methods is not able to correct for the deficiencies in the CASSCF reference wave function. The SA-CASSCF wave function, on the other hand, describes both boron atoms equivalently, i.e., the wave function describes an ''average'' of the resonance configurations B*–N–B$\leftrightarrow$B–N–B*. The SA-CASSCF+PT2 and CASSCF +1+2 methods include higher-order correlation effects without affecting the equivalency of the boron atoms.

ACKNOWLEDGMENTS

This work was performed in part at the Joint Institute for Computational Sciences, University of Tennessee–Oak Ridge National Laboratory. Support was provided by the Distinguished Scientist Program at the University of Tennessee and Oak Ridge National Laboratory. Oak Ridge National Laboratory is managed by UT-Battelle, LLC for the U.S. Department of Energy under Contract No. DE-AC05-00OR22725.

[1] P. B. Mirkarimi, K. F. McCarty, and D. L. Medlin, Mater. Sci. Eng. **21**, 47 (1997).
[2] S. Becker and H.-J. Dietze, Int. J. Mass Spectrom. Ion Processes **73**, 157 (1986).

[3] G. Seifert, B. Schwab, S. Becker, and H.-J. Dietze, Int. J. Mass Spectrom. Ion Processes **85**, 327 (1988).
[4] J. M. L. Martin, J.-P. François, and R. Gijbels, J. Chem. Phys. **90**, 6469 (1989).
[5] J. M. L. Martin, J.-P. François, and R. Gijbels, Chem. Phys. Lett. **172**, 354 (1990).
[6] L. B. Knight, Jr., D. W. Hill, T. J. Kirk, and C. A. Arrington, J. Phys. Chem. **96**, 555 (1992).
[7] J. M. L. Martin, J.-P. François, and R. Gijbels, Chem. Phys. Lett. **193**, 243 (1992).
[8] P. Hassanzadeh and L. Andrews, J. Phys. Chem. **96**, 9177 (1992).
[9] L. Andrews, P. Hassanzadeh, T. R. Burkholder, and J. M. L. Martin, J. Chem. Phys. **98**, 922 (1993).
[10] C. A. Thompson and L. Andrews, J. Am. Chem. Soc. **117**, 10125 (1995).
[11] C. A. Thompson, L. Andrews, J. M. L. Martin, and J. El-Yazal, J. Phys. Chem. **99**, 13839 (1995).
[12] J. M. L. Martin, J. El-Yazal, J.-P. François, and R. Gijbels, Mol. Phys. **85**, 527 (1995).
[13] Z.-X. Wang, M.-B. Huang, and P. von Ragué Schleyer, J. Phys. Chem. A **103**, 6475 (1999).
[14] (a) K. R. Asmis, T. R. Taylor, and D. M. Neumark, Eur. Phys. J. D **9**, 257 (1999); (b) K. R. Asmis, T. R. Taylor, and D. M. Neumark, J. Chem. Phys. **111**, 8838 (1999).
[15] G. Meloni, M. Sai Baba, and A. Gingerich, J. Chem. Phys. **113**, 8995 (2000).
[16] S. R. Gwaltney and M. Head-Gordon, Phys. Chem. Chem. Phys. **3**, 4495 (2001).
[17] S. Mahalakshmi and D. L. Yeager, Mol. Phys. **101**, 165 (2003).
[18] E. R. Davidson and W. T. Borden, J. Phys. Chem. **87**, 4783 (1983).
[19] I. B. Bersuker, Chem. Rev. **101**, 1067 (2001).
[20] T. H. Dunning, Jr., J. Chem. Phys. **90**, 1007 (1989).
[21] MOLPRO, a package of *ab initio* programs designed by H.-J. Werner and P. J. Knowles, version 2002.6, R. D. Amos, A. Bernhardsson, A. Berning *et al.*
[22] H. Bredohl, I. Dubois, Y. Houbrechts, and P. Nzohabonayo, J. Mol. Spectrosc. **112**, 430 (1985).
[23] K. A. Peterson, J. Chem. Phys. **102**, 262 (1995).
[24] K. R. Asmis, T. R. Taylor, and D. M. Neumark, Chem. Phys. Lett. **295**, 75 (1998).
[25] M. Lorenz, J. Agreiter, A. M. Smith, and V. E. Bondybey, J. Chem. Phys. **104**, 3143 (1996).